CHAPTER VIII
A STUDY ON ELECTRICALLY CONDUCTIVE BLENDS OF POLYCARBONATE/ LIQUID CRYSTALLINE POLYMER/ MULTI-WALLED CARBON NANOTUBES

8.1 Abstract

A thermotropic liquid crystalline polymer (LCP) was introduced into the composites of polycarbonate (PC) and multi-walled carbon nanotube (CNT) with the goal of improving electrical conductivity and mechanical properties. It was hypothesized that double percolation networks would be produced first from aligned, continuous fibrils of LCP and then by CNT networks within LCP fibrils. Two grades of LCP were chosen: Vectra A950 (VA950), and Vectra V400P (V400P) from Hoechst Celanese. The CNT used was Baytubes, C-150P and the PC used was Lexan 121. The compounds were prepared by melt-blending in a twin-screw mini-compounder and injection molded using a mini-injection molder. The LCP content was kept at 20 wt% and the CNT contents were varied from 0.5 to 15 wt%. Only PC/VA950 blend showed fibrils of LCP. However, these fibrils turned into droplets with the addition of CNT. Results from TEM showed that CNT preferentially located inside the LCP domains as predicted from the value of spreading coefficient. The electrical conductivity showed the following order (the numbers in parenthesis are electrical percolation threshold): PC/CNT (2%) > PC/VA950P/CNT (3%) > PC/VA400P/CNT (4%). The resulting discontinuity of the LCP droplet phase with CNTs located inside disrupted the electrically conductive pathways and resulted in lower electrical conductivity values. The value of storage modulus showed improvement by the addition of CNT and VA950.

Key words: Double Percolation; In-Situ Composites; Liquid Crystalline Polymer; Multi-Walled Carbon Nanotube

8.2 Introduction

Over the last two decades, blends of thermoplastic polymers with liquid crystalline polymer (LCP) received considerable interests from both academic and industrial researchers. The dispersed LCP domains tend to elongate during melt processing and subsequently form aligned fibrils capable of reinforcing the polymer matrix. The aligned fibril formation in these 'in situ composites' greatly depend on the choice of polymer matrix and selection of proper processing conditions. The formation of droplets, short fibrils, networks, and continuous fibrous LCP structures in a thermoplastic have also been reported. The research on in situ composites mainly dealt with unique morphology and consequent enhancement of mechanical properties, while those concerning the electrical properties are limited [1-3]. Carbon nanotubes (CNTs) offer excellent electrical properties, thermal conductivity, and mechanical strength although high cost and limited availability get in the way of developing widespread applications. Immiscible polymer blend systems have been effectively used in production of conductive composites via preferential localization of the conductive filler, e.g., carbon black, in one of the available phases. This so-called "double percolation" concept might be exploited to develop electrically conductive in situ composites of LCP. We hypothesized that the selective localization of CNTs in the continuous LCP fibrils would facilitate the anisotropic electrical conductivity, reduce the electrical percolation threshold, and enhance the melt processibility. LCP continuous fibrils have been observed in polycarbonate (PC) [4], polypropylene [5], poly(ether imide) [6] and Nylon 66 [7] with LCP content in the range 15-35%. In this contribution, the rheological, morphological, electrical and mechanical properties of the PC/LCP/CNT composites were studied. The structural changes in the blends caused by introducing CNTs were related to the viscosity changes and the consequent reduction of electrical conductivity.

8.3 Experimental

8.3.1 Materials

Polycarbonate (Lexan 121) was supplied by (SABIC). Two grades of LCPs; VA950 and VA400P were obtained from Hoechst Celanese. The CNT (diameter 13 nm, length > 1 μm) was obtained from BayerMaterialScience in the form of Baytubes, C-150P.

8.3.2 Composite Preparation

Compounds were prepared by melt-mixing in a twin-screw mini-compounder (Thermo Haake) at 290°C for neat PC and PC/V400P/CNT, and at 300°C for PC/ VA950/CNT, with a rotational speed of 60 rpm.

Injection-molded samples were prepared using a mini-injection-molding machine from DSM Research Netherlands with the injection-molding temperature/mold temperature of 310/150°C for PC, V400P and PC/ V400P/ CNT, 300/80°C for VA950 and PC/ VA950/ CNT, and the injection pressure of 6 bar for all samples. Injection-molded rectangular bars were cut into the dimensions of 36.0 x 12.0 x 2.0 mm^3 and 30.0 x 6.5 x 2.0 mm^3 for the determination of electrical conductivity and dynamic mechanical properties, respectively. PC, VA400P, and VA950 discs of diameter 2.8 mm, thickness 0.8 mm were used in contact angle measurements.

8.3.3 Characterization

The rheological properties of the samples were investigated using ARES, TA instruments. The frequency sweep measurement was performed with 25 mm parallel plate geometry, in oscillatory shear mode, and a fixed strain amplitude of 2%. A Rame-Hart contact angle goniometer (model 100-00) operating at 1 atm and a temperature of 24±2°C was used for measurement of contact angle of two reference liquids, diiodomethane and water. A Keithley Sub-Femtoamp Remote SourceMeter four-point conductivity probe (model 6430) was used for measurement of electrical conductivity of

the compounds with a current of 10 μA for low resistivity samples and a voltage of 100 V for high resistivity samples. The morphology of LCP was analyzed by scanning electron microscopy (SEM, JEOL SM-71510) and transmission electron microscopy (TEM, Tecnai 12 TEM). The LCP residue was obtained by immersing the blends in chloroform at room temperature for 12 h to dissolve all PC. The dynamic mechanical analyzer (RSA III) was used to study the mechanical response of the samples at temperature ranging from 35°C to 200°C and a heating rate of 4°C/ min. Tests were conducted in single point bending mode with a fixed strain of 0.2% and a vibration frequency of 1 Hz.

8.4 Results and Discussion

8.4.1 Melt Rheology

The melt rheological response during the frequency sweep was performed at two temperatures according to the injection molding conditions, i.e. 300°C for the systems comprising of VA950, and at 310°C for those comprising of V400P. From Figs 8.1 (a) and (b), It was found that at both temperatures, the neat PC showed Newtonian behavior and both LCPs exhibited non-Newtonian behavior, i.e. the complex viscosity (η^*) decreased with increasing frequency. It is widely accepted that the fibril formation of the LCP in a thermoplastic matrix is governed by two major factors: the ratio of viscosity of LCP to that of the matrix polymer and the interfacial tension between the polymer components. The LCP with lower viscosity than the matrix tends to elongate. In other words, the viscosity ratio of less than unity is promising for fibrillation of the LCP phase. In addition, sufficiently low interfacial tension between LCP and the matrix polymer is also required for good fibril formation. Also, the LCP content must be high to yield substantially large LCP domains that would facilitate the elongation process. It was found that the values of η^* of VA950 at 300°C were slightly greater than those of PC at very low frequencies (from 0.1 to 0.8 rad/s), and lesser at higher frequencies (from 0.8 to 100 rad/s), indicating that viscosity ratio of VA950 to PC would be less than unity

during injection molding. The blend of PC with 20 wt% VA950 showed viscosity higher than the individual polymer components. This can be attributed to transesterification at the interfaces of PC and VA950 as observed by Tovar *et al.* [8]. It is not surprising that the viscosity increased in compounds with the addition of CNTs. The viscosity of PC/VA950 with 5 wt% CNT was slightly lower than PC with 5wt% CNT and was greater than VA950 with 5 wt% CNT. At 310°C, V400P exhibited the upward concavity at low frequency which is often found in LCP. V400P LCP also showed higher viscosity than PC and, therefore, was expected to form spheres instead of fibrils in PC. As expected, the viscosity increased in presence of CNT. The viscosity of PC/V400P with 5 wt% CNT was found to be lower than the composites of the corresponding polymer components containing 5 wt% CNT. This can be attributed to the lubricating effect of the V400P domains.

8.4.2 Calculation of the Spreading Coefficient

The two-liquid geometric model was used to calculate the surface energy (Eq.8.1) [9,10] of the polymeric solids with the aid of contact angle measurements.

$$\gamma_{LV}(1+\cos\theta) = 2\left(\gamma_S^d \gamma_{LV}^d\right)^{1/2} + 2\left(\gamma_S^p \gamma_{LV}^p\right)^{1/2} \qquad (8.1)$$

In Eq. 8.1, γ_{LV} and γ_S are the surface energies of the reference liquid and the polymer respectively, the superscript d refers to the dispersion part and p refers to the polar part, and θ is the measured contact angle. It should be noted that the surface energy is the sum of the dispersion and the polar parts:

$$\gamma = \gamma^d + \gamma^p \qquad (8.2)$$

The interfacial energies can be calculated from the surface energies using two widely-used methods - the geometric-mean equation (Eq.8.3) and the harmonic-mean equation (Eq.8.4) [11];

$$\gamma_{12} = \gamma_1 + \gamma_2 - 2\left(\sqrt{\gamma_1^d \gamma_2^d} + \sqrt{\gamma_1^p \gamma_2^p}\right) \qquad (8.3)$$

$$\gamma_{12} = \gamma_1 + \gamma_2 - 4\left(\frac{\gamma_1^d \gamma_2^d}{\gamma_1^d + \gamma_2^d} + \frac{\gamma_1^p \gamma_2^p}{\gamma_1^p + \gamma_2^p}\right) \qquad (8.4)$$

where γ_i stands for the surface energy of the component i, γ_i^d and γ_i^p are the dispersive part and the polar part, respectively. A fairly successful approach to predict the morphology of the blends with a matrix component and two dispersed components was proposed by W.D. Harkins [12]. The Harkins' equation predicts the tendency of a liquid to spontaneously spread across the solid or liquid substrate using interfacial tension data. It was proposed in a three component system that component 3 encapsulates component 1 if the spreading coefficient , λ_{31} is positive:

$$\lambda_{31} = \gamma_{12} - \gamma_{32} - \gamma_{13} \qquad (8.5)$$

In Eq. 8.5, the three terms on the right are the interfacial energies between the respective components. Table 8.1 shows the contact angle values measured with diiodomethane and water, which were used to calculate the surface energy values reported in Table 8.2 using γ_{LV}^d and γ_{LV}^p of the reference liquids provided by Kaelble [13]. Although there was some disagreement in the literature for the contact angle data for PC [14] and VA950 [15,16], those values still cover our experimental values. The surface energy of V400P has not yet been reported by others and the values for CNT were taken from Ref. [17]. The polarity of the material was ranked as follows:CNT>V400P>VA950>PC. Since the carbonaceous materials tend to localize in more polar polymers [18], we anticipated that CNT would migrate towards the LCP phase. The interfacial energy of PC/VA950 was much lower than that of PC/V400P (see Table 8.3) suggesting that the former should be a more compatible blend than the latter. By considering CNT as component 1, PC as component 2, and LCP as component 3, and after substituting the interfacial energy values in Harkin's equation, the spreading coefficients of PC/V400P/CNT and PC/VA950/CNT were found to be 0.92 and 1.45 mJ/m^2 respectively. The positive λ_{31} value indicated the encapsulation of carbon nanotubes by the LCP. It should be noted that, in this contribution, all the surface tension data were obtained at room temperature instead of the processing temperature. It was considered that the changes in surface tension of most polymers with respect to temperature were comparable, e.g., 0.06-0.08 dyne·cm deg^{-1} [11,19,20].

8.4.3 Morphology

SEM images of LCP residue extracted from PC/V400P and PC/VA950 blends are presented in Fig. 8.2. The V400P phase in injection molded specimens remained in the form of droplets with the number-average diameter of 0.61 μm and a weight-average diameter of 0.67 μm [Fig. 8.2 (a)] as a result of lower viscosity of PC.

The as-compounded PC/VA950 blends taken from the mini-compounder also show spherical VA950 domains with number-average diameter of 0.49 μm and a weight-average diameter of 0.60 μm [Fig. 8.2(b)]. The VA950 domains in both fibrillar and spherical forms were found in injection molded specimen as in Fig. 8.2 (c). The pressure generated in the mini-injection molder probably was not high enough to obtain complete fibril formation. The all spherical domains resulted with the addition of 5 wt% CNT, Figs. 8.3(a) and (b). The surface of the droplets became rough as a result of the presence of LCP-coated CNT of ~50 nm diameter, although the diameter of pristine nanotube was reported to be 13 nm. The mixing sequence was found to influence both the size and shape of the LCP phase morphology. For example, larger and irregular dispersed VA950 domains resulted when CNT was first added into VA950 [Fig.8.3 (c)] compared to those of the reversed mixing sequence [Fig. 8.3 (b)].

Fig. 8.4 shows the TEM micrographs of the PC/CNT and PC/ LCP/ CNT composites. All the samples contain the same weight composition of 5 wt% CNT. The PC/CNT composite shows good CNT dispersion [Fig. 8.4 (a)] whereas PC/LCP/CNT composites [Figs. 8.4 (b) and (c)] clearly reveal non-uniform CNT dispersion. The darker areas in the form of sphere or ellipsoids are actually the LCP domains. Clearly, CNTs mainly resided inside the LCP droplets, in agreement with the SEM images seen in Fig. 8.3. There is no noticeable difference between composites PC/VA950/5 wt%CNT and PC/ V400P/5 wt%CNT. It will be shown later that their electrical conductivities at 5 wt% CNT loading were also found to be similar.

8.4.4 Electrical Conductivity

Fig. 8.5 provides the specific electrical conductivity of five compounds as function of CNT content. The electrical conductivity at 5 wt% CNT can be expressed in the following order with the numbers in parentheses representing electrical percolation threshold: PC/CNT (2%) > PC/VA950P/CNT (3%) > PC/V400P/CNT (4%). In light of the SEM and TEM images presented in Figs. 8.3 and 8.4, it can be inferred that the nanotube conductive pathways were destroyed in the presence of either type of the LCP and the shift in the percolation threshold to the higher CNT loading was observed. The composites of LCP and CNT were found to be insulators even when the CNT content was as high as 10 wt%. Thus, the strong insulating properties of an LCP and the tendency of CNT to localize in the LCP-phase lowered the values of electrical conductivity when incorporated into the PC/CNT compounds.

8.4.5 DMA Results

Table 8.4 shows the storage modulus at 40°C of three groups of sample; the neat polymer (PC, LCP), the neat blends of PC with 20 wt% LCP, and the composites of 5 wt% CNT (PC/CNT, LCP/CNT, PC/LCP/CNT).

The storage moduli at less than 110°C of compounds containing V400P showed the following order: V400P/CNT > V400P > PC/V400P > PC/CNT > PC > PC/V400P/CNT. For VA950-containing compounds, the storage moduli at low temperature show the following trend: VA950/CNT > VA950 > PC/VA950/CNT > PC/VA950 > PC/CNT > PC.

8.5 Conclusions

In this study, the PC/LCP/CNT composites were investigated in an attempt to utilize the double percolation concept to improve the electrical conductivity. Without CNT, VA950 formed fibrils whereas V400P existed as droplets in the PC matrix which is in good agreement with the rheological data. For both LCPs, CNT particles were preferentially located inside the LCP domains as predicted by the positive values of the

spreading coefficient parameter. Such localization caused the viscosity of the LCP domains to rise and thus impede the deformation of the LCP phase during injection molding. The discontinuous LCP phase disrupted the CNT conductive pathways and shifted the electrical percolation to higher CNT content. As a result, the application of the double percolation model was not successful.

8.6 Acknowledgements

This work was supported by a grant from the Thailand Research Fund (TRF-RGJ Program), The Petroleum and Petrochemical College, and National Excellence Center for Petroleum, Petrochemical, and Advanced Materials.

8.7 References

1. R. Tchoudakov, M. Nakis, and A. Seigmann, *Polym Eng Sci,* **44**, 528-540 (2004).

2. Y.W. Wong, K. L. Lo, and F. G. Shin, *J Appl Polym Sci,* **82**, 1549-1555 (2001).

3. J. Bao, C. Xu, W. Cai, and X. T. Bi, *J Appl Polym Sci*, **52**, 1489-1497 (1994).

4. L.P. Tan, C.Y. Yue, K.C. Tam, Y.C. Lam, and X. Hu, *Polym Int*, **51**, 398-405 (2002).

5. H.H. Chen, J.P. deSouza, D.G. Baird, K.T. The, and J. Morton. *ICCM/ 9* , **5**, 456-460 (1993).

6. A.I. Isayev, and S. Swaminathan. Tchoudakov, M. Nakis, and A. Seigmann, U.S. Patent 4,835,047 (1989).

7. H. Wang, K.W. Lee, T.S. Chung, and M. Jaffe, *Polym Compos,* **21**, 114-123 (2000).

8. G. Tovar, P.J. Carreau, and H.P. Schreiber, *Colloids Surf*, **161**, 213-223 (2000).

9. D.K. Owens, and R.C. Wendt, *J Appl Polym Sci*, **13**, 1741-1747, (1969).

10. D.H. Kealble, *J Adhesion*, **2**, 50-60, (1970).

11. S. Wu, *Polymer Interface and Adhesion*, Marcel Dekker, New York (1982).

12. W.D. Harkins, *The Physical Chemistry of Surface Films*, Reinhold Pub. Co., New York, (1952), p.23.

13. D.H. Kaelble, *Physical Chemistry of Adhesion*, Wiley Interscience, New York, (1970), p. 149.

14. http://www.accudynetest.com/polymer_surface_data/polycarbonate.pdf.

15. K.X. Ma, T.S. Chung, and R.J. Good, *J Polym Sci Part B: Polym Phys*, **36**, 2327-2337, (1998).

16. T.S. Chung, K.X. Ma, and M. Jaffe, *Macromol Chem Phys*, **199**, 1013-1017, (1998).

17. S. Nuriel, L. Liu, A.H. Barber, and H.D. Wagner, *Chem Phys Lett*, **404**, 263-266, (2005).

18. R.A. Ryntz, and P.V. Yaneff, *Coatings of polymers and plastics*, Marcel Dekker, New York, (2003), p. 43.

19. S. Wu, *J Polym Sci C*, **34**, 19-30, (1971).

20. G.L. Gaines, *Polym Eng Sci*, **12 (1)**, 1-11, (1972).

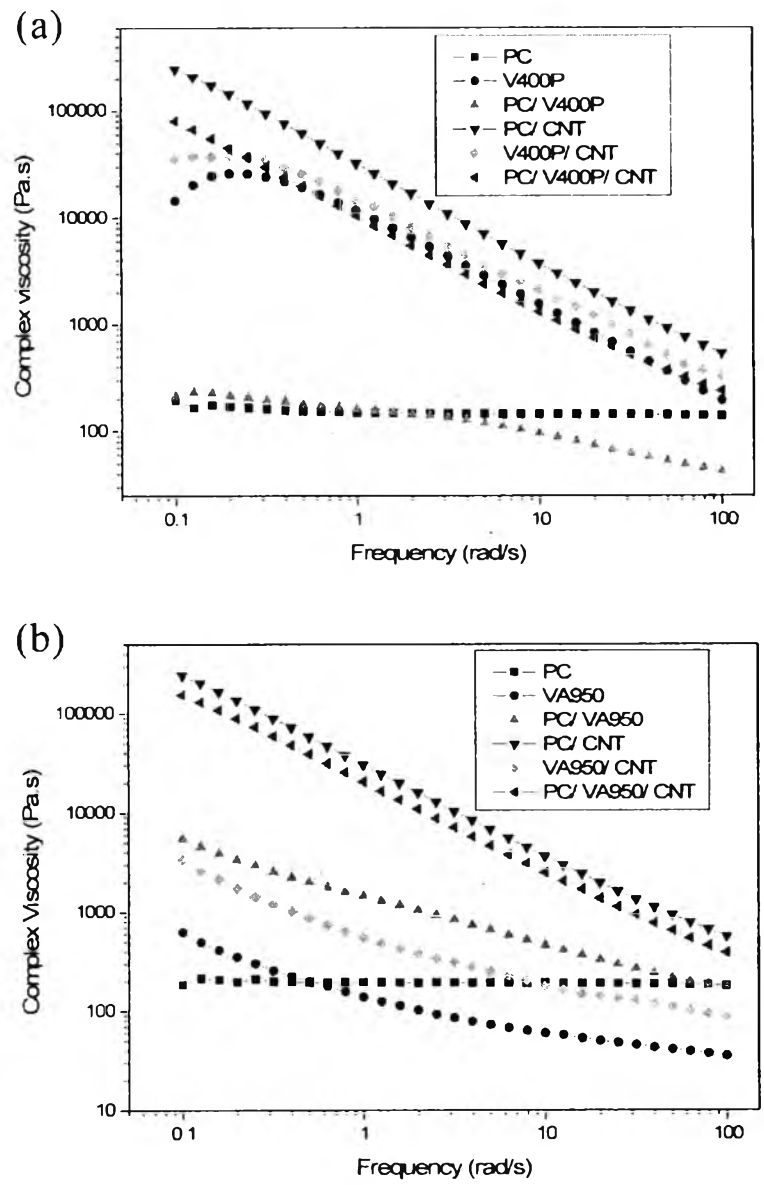

Figure 8.1 Comparison of complex viscosity for PC, PC/ LCP blends, and composites with 5 wt% CNT where the LCP used is V400P (measured at 310°C) (a), and VA950 (measured at 300°C) (b).

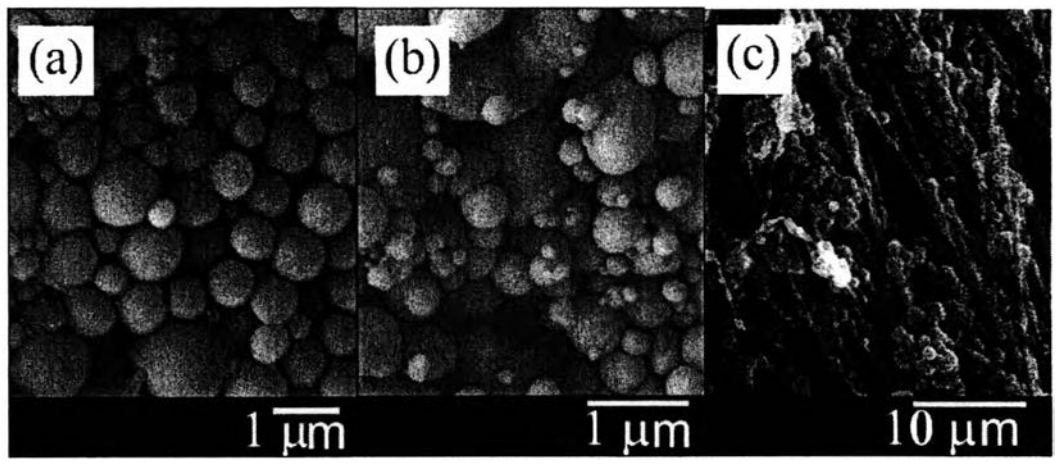

Figure 8.2 SEM micrographs of the LCP residues of PC/V400P injection-molded specimen (a), as-compounded PC/VA950 (b), and PC/VA950 injection-molded specimen (c).

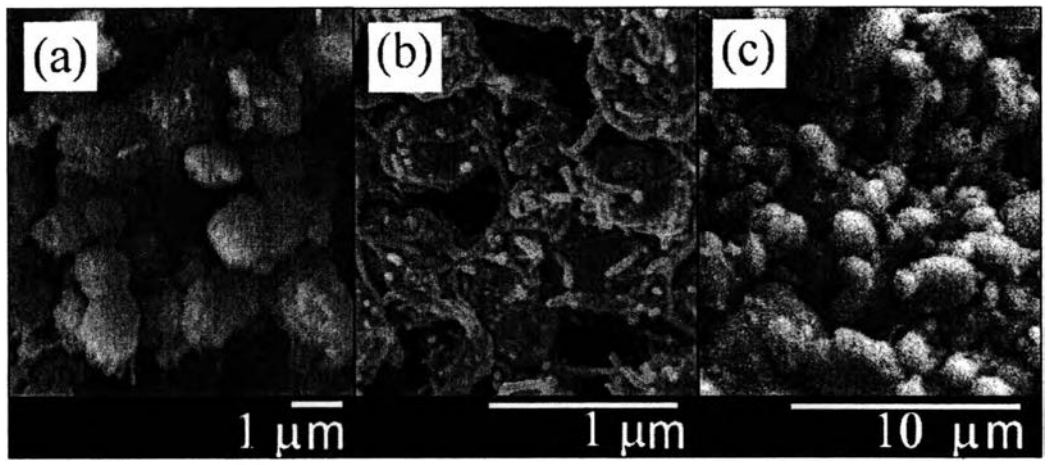

Figure 8.3 SEM micrographs of the LCP residues of the injection-molded specimen of PC/V400P/5wt%CNT (a), PC/VA950/5wt%CNT (b), PC/VA950/5wt% CNT with reversed feeding sequence (c).

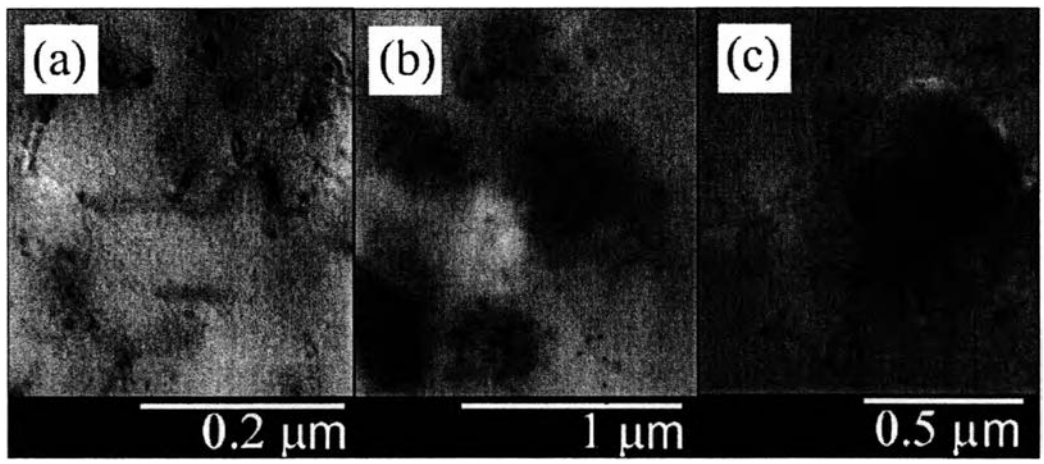

Figure 8.4 TEM micrographs of the thin sections of 5 wt% CNT composites based on the neat PC (a), PC/ V400P (b), and PC/ VA950 (c).

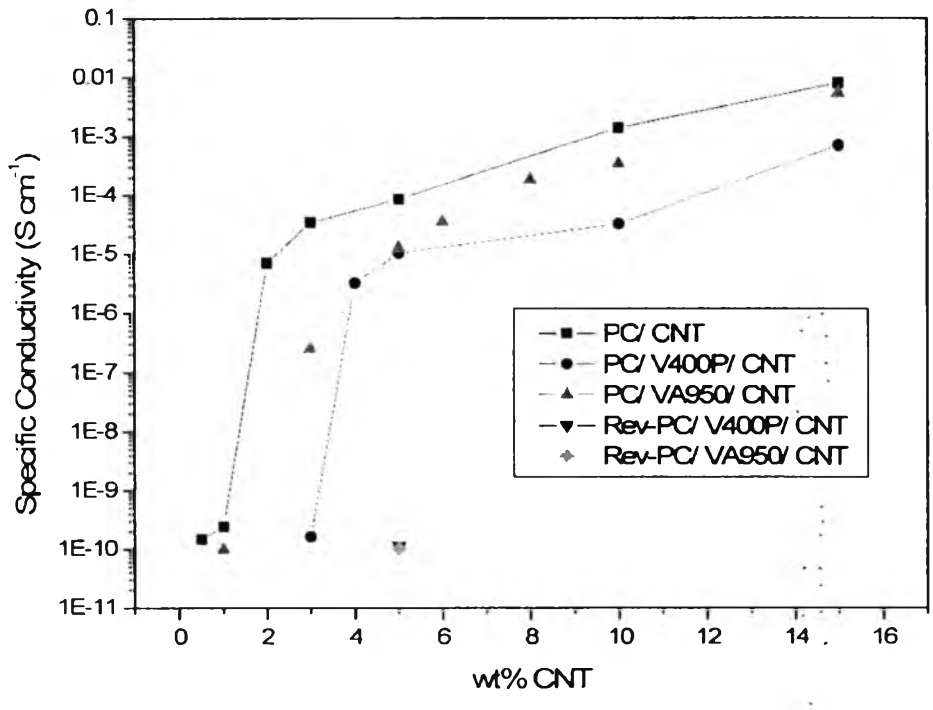

Figure 8.5 The volume conductivity as a function of CNT concentration.

Table 8.1 Contact angle determination on polymers

Material	Contact Angle (Degree)	
	Diiodomethane	Water
PC	29.2	72.2
V400P	25.3	60.0
VA950	29.9	70.0

Table 8.2 Surface energies (in mJ/m^2) based on the two-liquid geometric method

Material	γ^d	γ^p	γ	Polarity (%)
PC	39.36	6.50	45.86	14.2
V400P	17.56	24.06	41.62	57.8
VA950	38.42	7.79	46.21	16.9
CNT	18.4	26.9	45.3	59.4

Table 8.3 Summary of interfacial energies calculated from the geometric-mean equation and the harmonic-mean equation

Material	Interfacial Energy (mJ/m^2)	
	Geometric-mean equation	Harmonic-mean equation
PC/CNT	10.89	20.06
V400P/CNT	0.09	0.18
VA950/CNT	9.38	17.58
PC/V400P	9.88	18.43
PC/VA950	0.06	0.13

Table 8.4 Storage moduli, G' at 40°C, for PC, PC/ LCP blends, and composites with 5 wt% CNT

Material	G' (GPa)
PC	1.58
PC/CNT	1.73
V400P	4.30
V400P/CNT	4.83
PC/V400P	2.25
PC/V400P/CNT	1.57
VA950	3.05
VA950/CNT	4.28
PC/VA950	1.74
PC/VA950/CNT	1.83